Journal of Petroleum Science and Engineering 72 (2010) 50–55

Contents lists available at ScienceDirect

Journal of Petroleum Science and Engineering

journal homepage: www.elsevier.com/locate/petrol

Viscous creep in room-dried unconsolidated Gulf of Mexico shale (II): Development of a viscoplasticity model

Chandong Chang [a,*], Mark D. Zoback [b,1]

[a] Department of Geology, Chungnam National University, Daejeon, 305-764, South Korea
[b] Department of Geophysics, Stanford University, Palo Alto, CA 94305-2215, USA

ARTICLE INFO

Article history:
Received 12 September 2008
Accepted 3 March 2010

Keywords:
creep
shale
viscoplasticity
plastic yield model
yield stress

ABSTRACT

Laboratory creep experiments show that compaction of dry Gulf of Mexico shale is a permanent irrecoverable process associated with viscoplastic deformation. In order to find a relatively simple model that can describe such viscoplastic behavior of the dry frame of the shale, we combined the Perzyna viscoplasticity constitutive law with a modified Cambridge clay plastic yield model. The constitutive equation for this model is a power-law function that relates strain rate to the ratio of dynamic and static yield surfaces defined by the modified Cam-clay model. By incorporating the effect of strain hardening on the static yield pressure, we derived an equation relating volumetric creep strain at a constant hydrostatic pressure level to the logarithm of time, which is in good agreement with experimental results. We determined the model parameters by fitting experimental data of creep strain as a function of time. The determined parameters indicate that the yield stress of the hydrostatically loaded shale increases by 6–7% as strain rate rises by an order of magnitude. This demonstrates that the laboratory-based prediction of yield stress (as well as porosity) may be significantly overestimated. Thus, strain-rate calibration is required for weak shales such as those studied here to appropriately estimate physical properties under in situ conditions.

1. Introduction

A laboratory study on creep strain of dry Gulf of Mexico shale revealed that time-dependent deformation is a significant intrinsic behavior of the dry frame of unconsolidated shale (Chang and Zoback, 2009). This is important because time-dependent shale compaction is typically only attributed to poroelastic effects (Cogan, 1976; Karig, 1993; Hornby, 1998).

In this paper, we attempt to quantitatively determine the time-dependent properties of the dry frame of the shale based on a relatively simple rheological model and thus incorporate this effect when modeling shale compaction. Previous studies employed viscoelastic rheological models to explain the time-dependent behavior of unconsolidated sands (Ostermeier, 1995; Chang et al., 1997; Hagin and Zoback, 2004a). Viscoelasticity theory has frequently been utilized in rock mechanics since these models were complex enough to describe many aspects of time-dependent characteristics and are readily applicable to experimental data. There are several reasons, however, that viscoelasticity theory may not be fully adequate to fully describe shale deformation. First, creep in the shale is irreversible permanent deformation. Second, the dynamic properties such as ultrasonic velocities and dynamic moduli evolve with time and remain almost the same when the sample is unloaded. These phenomena indicate that there is a significant strain- or work-hardening effect in the viscous deformation of shale, which implies that shale deformation is viscoplastic.

Since Perzyna (1963) suggested a theoretical framework for elasto-viscoplastic deformation, several constitutive models have been suggested that are suitable for describing the rate-sensitive, viscous behavior of soils and clays (Adachi and Oka, 1982; Katona, 1984; Kutter and Sathialingam, 1992; Yin and Graham, 1999; Namikawa, 2001). These models were developed primarily to explain consolidation of saturated soil, in which pore pressure dissipation was considered as a major source of time-dependent deformation. Obviously the viscoplastic parameters evaluated from these models would wind up modeling effects of material properties and material–pore fluid coupling.

The same theoretical approach taken by the previous studies can be utilized in order to quantitatively characterize viscous properties of the dry skeleton of the shale, which involves material properties that are isolated from the poroelastic effect. In the present study, we follow the approach first suggested by Adachi and Oka (1982) and later modified by Namikawa (2001), both of whom combined Perzyna's viscoplasticity theory with the original Cambridge clay plastic end-cap model (Roscoe et al., 1963). We use a modified Cam-clay model because it is analytically simple but still gives a good

* Corresponding author. Tel.: +82 42 821 6430; fax: +82 42 823 5636.
E-mail addresses: cchang@cnu.ac.kr (C. Chang), zoback@stanford.edu (M.D. Zoback).
[1] Tel.: +1 650 725 9295; fax: +1 650 725 7344.

0920-4105/$ – see front matter © 2010 Elsevier B.V. All rights reserved.
doi:10.1016/j.petrol.2010.03.002

prediction of plastic strain as well as porosity change under both shearing and compaction (Roscoe and Burland, 1968; Desai and Siriwardane, 1984). The fundamental idea then, is to recast the inviscid Cam-clay model into the viscoplasticity theory so as to permit a unified description of strain hardening and rate-sensitive plastic behavior of unconsolidated materials. Our primary focus is to document and model the time-dependent deformation, and not to produce a full constitutive law for the shale samples.

2. Summary of laboratory observations on creep

We summarize here observations from our laboratory experiments on room-dried unconsolidated Gulf of Mexico shale. A detailed explanation of our experiments and results can be found in the companion paper (Chang and Zoback, 2009). In short, we conducted a series of hydrostatic pressure experiments in which pressure was raised in 5 MPa steps from 10 MPa to 50 MPa and at each step it was kept constant for 6 h. The shale exhibited a pronounced time-dependent creep at all constant stress levels during an elevated loading path. The creep strain at constant stress was fit by a logarithmic function of time. The contribution of creep to shale compaction was significantly larger than that of instantaneous loading. The creep strain for 6 h associated with an instantaneous 5 MPa loading ramp was as high as ~6 times of the corresponding instantaneous strain. Porosity loss and increases in dynamic moduli of the shale were observed during creep. In all tests, the shale exhibited a lack of creep (and nearly negligible strain recovery) when unloaded, suggesting that the creep process in the shale is largely unrecoverable with unloading. This implies that creep strain is best described as viscoplasticity.

The creep behavior in the shale depends on the magnitude of the applied pressure (or stress). The amount of creep at a constant pressure level after a given time was seen to increase linearly with equal incremental pressure steps up to ~30 MPa. Thus, the total cumulative creep strain accelerated nonlinearly as pressure increased in this pressure range. When the pressure was increased in equal steps beyond ~30 MPa, the amount of creep at a constant pressure level after a given time was nearly constant, suggesting that in this relatively high-pressure regime, creep characteristics obey a linear viscous rheology as found by Hagin and Zoback (2004a) for unconsolidated sands.

3. Perzyna's elasto-viscoplasticity theory

A number of viscoplastic models have been developed based on the elastic-viscoplastic modeling framework of Perzyna (1963). The foundation of Perzyna's theory is based on the premise that a total strain rate $\dot{\varepsilon}$ is decomposed into elastic (instantaneous) strain rate $\dot{\varepsilon}^{e}$ and viscoplastic strain rate $\dot{\varepsilon}^{vp}$. While the elastic portion of strain rate is defined simply by Hooke's law, the viscoplastic strain rate is accounted for by the following flow rule:

$$\dot{\varepsilon}_{ij}^{vp} = \langle \varphi(F) \rangle \frac{\partial f_d}{\partial \sigma_{ij}} \tag{1}$$

where φ is the viscoplastic flow function, F is the overstress function, and $\langle\rangle$ is MacCauley's bracket, with which $\langle \varphi(F) \rangle = 0$ for $F \leq 0$ and $\langle \varphi(F) \rangle = \varphi(F)$ for $F>0$. The explicit form of φ can be obtained experimentally or theoretically. The function f_d is the dynamic yield function, which depends on the current state of stress. Perzyna pointed out that the difference of the dynamic and static behaviors of material occurred due to the strain-rate sensitivity of the material and defined this rate-sensitive behavior as viscoplastic. From his assumption, the overstress is defined as a normalized distance between the current stress and the stress on the static yield surface:

$$F = \frac{f_d - f_s}{f_s} = \frac{f_d}{f_s} - 1 \tag{2}$$

where f_s is the static yield function that accounts for plastic strain hardening. If the current state of stress is less than the static yield stress (i.e. $F \leq 0$), the material behaves elastically ($\dot{\varepsilon}^{vp} = 0$), but after the current stress exceeds the static yield stress, viscoplastic strain occurs at a rate defined by Eq. (1).

While many investigators proposed a variety of functional forms of φ, there is no standard mathematical method to obtain its specific form. In our study, we use a power-law function because it has been found by a number of previous studies to derive reasonably good results (Kutter and Sathialingam, 1992; Fodil et al., 1997; Vermeer and Neher, 1999; Hagin and Zoback, 2004b). As used by these studies, φ takes the form of

$$\varphi = c_o \left(\frac{f_d}{f_s} \right)^n \tag{3}$$

where c_o and n are two material constants. Thus, the viscoplastic strain rate has the form of

$$\dot{\varepsilon}_{ij}^{vp} = c_o \left(\frac{f_d}{f_s} \right)^n \frac{\partial f_d}{\partial \sigma_{ij}}. \tag{4}$$

As we will show later, the selection of a power-law function for φ enables us to analytically derive the viscoplastic creep strain as a function of time, which is necessary to determine the model parameters.

4. Yield functions

In order to specify the viscoplastic constitutive Eq. (4), it is necessary to define the static and dynamic yield functions, f_s and f_d. The static yield function defines the critical stress for a perfectly elastic–plastic material, while the dynamic yield function defines the equivalent for a viscoplastic material. The yield functions for unconsolidated geomaterials such as sands, shales and other types of soil have been derived in the form of cap-type constitutive equations in order to describe plastic strain and porosity change associated with compaction and consolidation. We utilize the modified Cam-clay model (Roscoe and Burland, 1968; Desai and Siriwardane, 1984) because of its relative simplicity. The yield surface of the modified Cam-clay model is an elliptical shape in $p-q$ space, which is expressed in the form of

$$M^2 p^2 - M^2 p_o p + q^2 = 0 \tag{5}$$

where p is the mean normal stress ($\equiv(\sigma_1+\sigma_2+\sigma_3)/3$), and q is the deviatoric stress $\left(\equiv \left((\sigma_1-\sigma_2)^2 + (\sigma_2-\sigma_3)^2 + (\sigma_3-\sigma_1)^2 \right)^{1/2} / \sqrt{2} \right)$; M is the slope of the critical state line in $p-q$ space; and p_o, known as the preconsolidation pressure, is the intersection between the static yield surface and p-axis. Two material parameters, M and p_o, fully define the yield surface. As shown in Fig. 1, the critical state line intersects the ellipse at its highest point, implying that M controls the ellipticity of the yield surface, while the preconsolidation pressure p_o determines the size of the yield surface.

If the stress state is within the domain bounded by the yield surface, the rock deformation is, by definition, elastic. If the stress state is outside the given yield surface, the rock compacts and undergoes plastic hardening. The plastic hardening is represented by an increase of p_o (from p_{o1} to p_{o2} in Fig. 1a), and subsequently the expansion of size of the yield surface. Because plastic deformation is associated with pore closure, it is often possible to relate preconsolidation pressures to porosities (Schutjens et al., 2004, for example). The value of p_o can be determined easily from a series of hydrostatic compression tests, in which porosity is measured as a function of confining pressure. Thus it is possible to characterize the yield

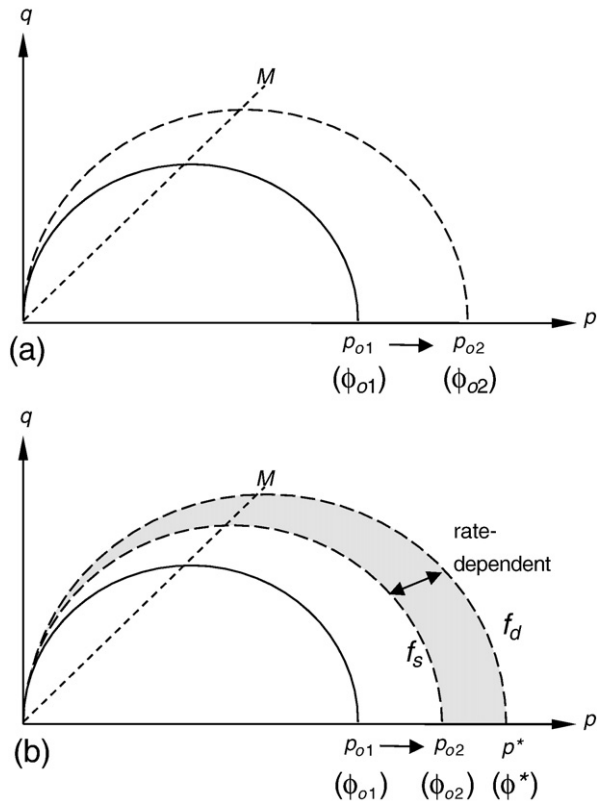

Fig. 1. Schematic illustration of the modified Cam-clay plastic model in $p-q$ space. (a) For elastic–plastic material, plastic compaction and the associated porosity reduction are represented by the increase of the preconsolidation pressure (from p_{o1} to p_{o2}) and a corresponding increase in size of the end-cap. (b) For elasto-viscoplastic material, the size of the ellipse (f_d) increases as strain rate increases. ϕ_{o1}, ϕ_{o2} and ϕ^* are porosities corresponding to the respective preconsolidation pressures, p_{o1}, p_{o2} and p^*.

surface as a function of p_o. By modifying Eq. (5), we obtain the static yield function f_s in the form of

$$f_s = p_o = p^{(s)} + \frac{\left(q^{(s)}\right)^2}{M^2 p^{(s)}} \tag{6}$$

where the superscript (s) denotes the stress condition on the static yield surface, in order to distinguish it from the stress condition along the dynamic yield surface (introduced below). As long as the material behavior is inviscid, a single value of p_o is correlated with a unique yield function that defines the boundary between elastic and plastic ranges.

If the material behavior is viscous (time- and rate-dependent), however, the size of the yield surface varies depending on strain rate even though the preconsolidation pressure is fixed (Fig. 1b). Thus, the relationship between porosity and the size of yield surface of the viscous material is not uniquely defined any more. Assuming that the form of the dynamic yield surface is similar to the static one, we can express the dynamic yield function f_d in the same form as the static yield function:

$$f_d = p^* = p + \frac{q^2}{M^2 p} \tag{7}$$

where p^* is the intersection between the dynamic yield surface and p-axis.

As implied by Eq. (4), a higher strain rate causes the yield surface (p^*) to be larger in size. Thus, conventional relatively high strain-rate laboratory experiments tend to overestimate the yield stress compared to in situ deformation rates (Fig. 1b). The significance of the rate effect on yield stress depends on viscoplastic material constants in the constitutive equation, in which viscoplasticity and Cam-clay model are combined. This is addressed in the next section.

5. Application of the viscoplasticity to isotropic consolidation

We applied the viscoplasticity theory in conjunction with the modified Cam-clay model to our hydrostatic pressure experimental results in order to model the viscoplastic behavior of the dry frame of GOM shale and to find the rate-dependency parameters. By combining Eqs. (4), (6) and (7), the viscoplastic volumetric strain rate is written as

$$\dot{\varepsilon}^{vp} = \dot{\varepsilon}_{11}^{vp} + \dot{\varepsilon}_{22}^{vp} + \dot{\varepsilon}_{33}^{vp} = c_o\left(\frac{f_d}{f_s}\right)^n\left(\frac{\partial f_d}{\partial \sigma_{11}} + \frac{\partial f_d}{\partial \sigma_{22}} + \frac{\partial f_d}{\partial \sigma_{33}}\right) = c_o\left(\frac{f_d}{f_s}\right)^n\left(1-\left(\frac{q}{Mp}\right)^2\right). \tag{8}$$

Eq. (8) is a generalized formulation of viscoplastic volumetric strain rate valid for any stress condition. For isotropic loading ($\sigma_1=\sigma_2=\sigma_3=p$, $q=0$), the static and dynamic yield functions are simplified to p_o and p ($=p^*$). Thus, the viscoplastic volumetric strain rate is simply in the form of

$$\dot{\varepsilon}^{vp} = c_o\left(\frac{p}{p_o}\right)^n. \tag{9}$$

It should be noted that in Eq. (9), the preconsolidation pressure p_o is not a fixed constant during deformation; it is a strain-dependent parameter due to strain hardening (Perzyna, 1963; Bjerrum, 1967). Fig. 2 depicts this concept using an idealized stress–strain curve in $\varepsilon-\ln p$ space as used in the conventional soil mechanics. When an elastic–plastic material (with its initial preconsolidation pressure p_{oi}) is compressed, it first deforms elastically (with the slope of the line being C_s called swelling index) until the pressure reaches the initial preconsolidation pressure, and thereafter it follows the inviscid normal compaction line (with the slope being C_c called compression index) as pressure increases further. As the rock experiences a plastic strain, the preconsolidation pressure evolves progressively, following the normal compaction stress–strain line. Thus, in the case of inviscid deformation, the normal compaction line can be considered as a locus along which the preconsolidation pressure evolves in the stress–strain domain.

The strain-hardening concept can be extended to the case of elasto-viscoplastic deformation. That is, the viscoplastic strain causes the

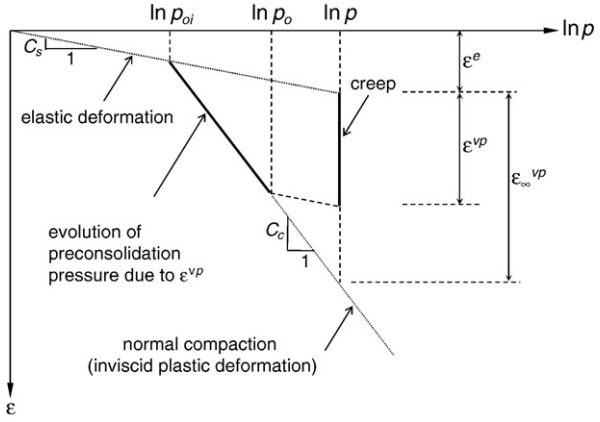

Fig. 2. Schematic of $\ln p-\varepsilon$ lines for the hydrostatic loading. When pressure is increased instantly to p, the elasto-viscoplastic material first deforms elastically (ε^e) and shows creep strain (ε^{vp}). During the creep, a progressive evolution of preconsolidation pressure occurs that follows the normal compaction line.

increase in preconsolidation pressure for elasto-viscoplastic material. As the viscoplastic strain is time-dependent, so is the evolution of preconsolidation pressure. In Fig. 2, the creep strain ε^{vp} that occurs at pressure p for a given period of time corresponds to the increase in preconsolidation pressure from p_{oi} to p_o. If creep continues with time, preconsolidation pressure keeps increasing until it reaches eventually the value of p. In Fig. 2, the relation between viscoplastic strain and preconsolidation pressure can easily be derived in the form of

$$\varepsilon_{\infty}^{vp} - \varepsilon^{vp} = (C_c - C_s)\ln\frac{p}{p_o} \tag{10}$$

where $\varepsilon_{\infty}^{vp}$ is the total viscoplastic strain at the end of consolidation at pressure p. The implication of Eq. (10) is that a total amount of viscoplastic strain ($\varepsilon_{\infty}^{vp} - \varepsilon^{vp}$) is expected when a material of preconsolidation pressure p_o is loaded hydrostatically to a pressure p ($>p_o$). Thus, if the pressure is increased instantaneously to pressure p, the creep strain as a function of time will follow the instantaneous loading. At the same time, the preconsolidation pressure will evolve with the creep strain ε^{vp}. In other words, it is possible to say that the creep strain is a result of time-dependent evolution of the preconsolidation pressure, and vice versa.

The viscoplastic strain associated with the time-dependent evolution of preconsolidation pressure can be described by a differential equation derived by combining Eqs. (9) and (10) and eliminating the p/p_o term,

$$\dot{\varepsilon}^{vp} = c_o e^{D\varepsilon_{\infty}^{vp}} e^{-D\varepsilon^{vp}} \tag{11}$$

where $D = n/(C_c - C_s)$. Solving the differential equation in order to obtain a time function of ε^{vp} requires an initial condition. Let us assume that at $t=0$, the preconsolidation pressure reaches p_o and that a total cumulative amount of viscoplastic strain that contributes to increase the preconsolidation pressure from p_{oi} to p_o is ε_o^{vp}. Using this initial condition, we obtain an analytic solution of the differential equation in the form of

$$\varepsilon^{vp}(t) = \frac{1}{D}\ln\left(c_o D e^{D\varepsilon_{\infty}^{vp}} t + e^{D\varepsilon_o^{vp}}\right). \tag{12}$$

Note that at $t=0$, Eq. (12) gives $\varepsilon^{vp}(0) = \varepsilon_o^{vp}$, which is viscoplastic strain accumulated before $t=0$. If we subtract the initial strain ε_o^{vp} from Eq. (12), we can obtain creep strain ε^c as a function of time that contributes to the increase of preconsolidation pressure from p_o to p, which is in the form of

$$\varepsilon^c = \frac{1}{D}\ln\left(c_o D e^{D\left(\varepsilon_{\infty}^{vp} - \varepsilon_o^{vp}\right)} t + 1\right). \tag{13}$$

When pressure is increased to a value of p instantaneously beyond the preconsolidation pressure p_o, the creep strain is expected to follow the time function given by Eq. (13). The use of Perzyna's viscoplastic theory in conjunction with the modified Cam-clay model thus estimates creep strain as a logarithmic function of time. This is in good agreement with our laboratory observation (Chang and Zoback, 2009). Thus, it is possible to determine the viscoplastic model parameters by comparing Eq. (13) with the laboratory creep strain results, as done in the next section.

6. Determination of model parameters

The viscoplastic model for isotropic loading condition requires the determination of four material constants: C_s, C_c, n, and c_o. The swelling index C_s can be relatively easily estimated from the unloading–reloading stress–strain curve, which is considered as the elastic portion of deformation (see Fig. 3). The measured value of C_s is 0.0074 ± 0.0021.

The determination of incremental volumetric plastic strain parameter C_c is difficult, because ideally one needs to run an experiment at an infinitesimal strain rate to avoid any time-dependent deformation and thus simulate pure inviscid deformation. This is virtually impossible at laboratory time-scales. However, Bjerrum (1967) showed that the slope of the normal compaction lines with different consolidation times are approximately parallel as long as the sustained time is kept consistent in a test, demonstrating that the slope is practically independent of the time of sustained loading. This notion alternatively indicates that if we use different consistent sustained time, the slope will remain unchanged. Thus, the value of C_c, a material property that defines the normal compaction line, can be obtained directly from the slope of the envelope of the $\ln(p) - \varepsilon$ line in the viscoplastic range (see Fig. 3 as an example). The average value of C_c estimates is 0.085 ± 0.010.

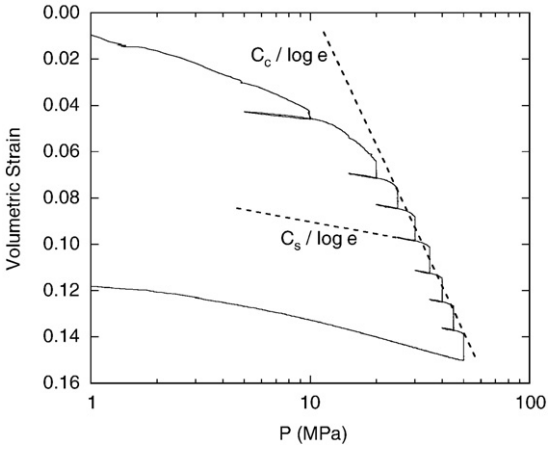

Fig. 3. An example showing how we determined the swelling index (C_s) and compression index (C_c).

Interestingly, our C_c estimate is remarkably similar to that determined from other independently measured result. Stump and Flemings (2002) presented a stress–strain curve (Fig. 4) measured in the GOM shale recovered from the pathfinder well (the same well, from which our shale sample was recovered) at a depth just 20 m above our shale sample. Their experiment was conducted under uniaxial strain condition (similar to oedometer test in soil mechanics) at a stress rate of 7×10^{-4} MPa/min. Because the stress ratio K_0 (lateral stress/vertical stress) in the plastic range (above yield point) was 0.85, the stress condition can be thought of as approximately hydrostatic. The slope of the normal compression line in their result

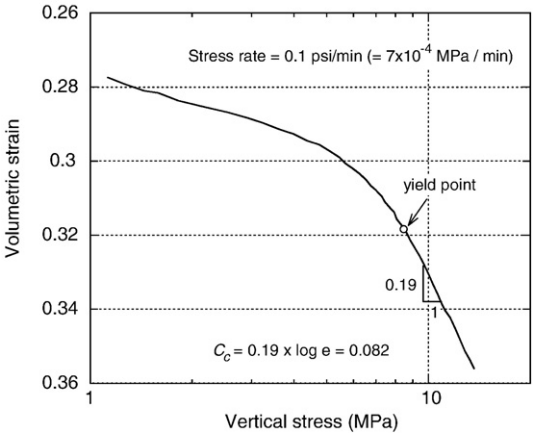

Fig. 4. Stress–strain curve (after Stump and Flemings, 2002) measured in a uniaxial strain experiment on GOM shale similar to that used by Chang and Zoback (2009). Note that beyond yield point the stress ratio between lateral and vertical stress is 0.85, which can be considered as approximately hydrostatic.

was 0.082, which coincides remarkably well with our estimation. We are not sure whether the close match between these values is entirely coincidental since we do not have other independent evidence showing that this section of the shale in the borehole is homogeneous. However, if the shale is homogeneous, the analogy between the two results provides a possibility to determine the C_c value with different techniques.

The other two viscoplastic parameters n and c_o were determined from the creep strain data as a function of time using Eq. (13). Note that in our creep experiments, we first applied rapid pressurization at a rate of 5 MPa/min and kept the pressure constant for about 6 h, during which creep strain was recorded as a function of time. We assume that the elastic and the viscoplastic portions of deformation were completely decomposed in our experiments. This means that when we increased the pressure almost instantaneously, we assume that the shale deformed elastically and only after keeping the pressure constant, the viscoplastic strain occurred. Since the unloading/reloading curves in our experiments were nearly linear, we believe that this is a reasonable assumption. In that way, the creep strain as a function of time is considered as a unique material viscoplastic strain–time curve at a given pressure.

While the rheology of the shale viscoplasticity consists of linear (above 30 MPa) and nonlinear (below 30 MPa) portions, we focus only on the linear portion of the rheology. We mean by linear that the viscoplastic strain is a linear function of stress. In Fig. 5, we plotted all the creep strain data that were measured at pressures above 30 MPa as a function of logarithm of time as implied by Eq. (13). Note that all the lines are nearly parallel one another. It is because the slope of the curve is determined by the coefficient $1/D=(C_c-C_s)/n$, which is a material property. From a regression analysis on the slope of the creep curves, the average value of n was determined to be 38 ± 4.

It is also noted in Fig. 5 that the positions of individual curves are slightly different. It is because the term of $(\varepsilon_\infty^{vp}-\varepsilon_o^{vp})$ in Eq. (13) is not a material constant, but has a value depending on the stress condition and the state of preconsolidation. This information gives a way to estimate the parameter c_o. It is noteworthy that obtaining an accurate value of c_o is not as important as that of n, since it is only a scale factor for the absolute value of viscoplastic strain rate (as implied by Eq. (9)). The relative effect of different strain rates on yielding is known from the value of n only.

Using Eq. (10), the term $c_oDe^{D(\varepsilon_\infty^{vp}-\varepsilon_o^{vp})}$ in Eq. (13) can be rewritten as $c_oD(p/p_o)^n$. Thus if we know the preconsolidation pressure p_o just before we raise the pressure to the next 5 MPa step, the parameter c_o can be determined by comparing the coefficient $c_oDe^{D(\varepsilon_\infty^{vp}-\varepsilon_o^{vp})}$ determined from the creep strain–time curves and the calculated value of $D(p/p_o)^n$. The correlation factor would be parameter c_o.

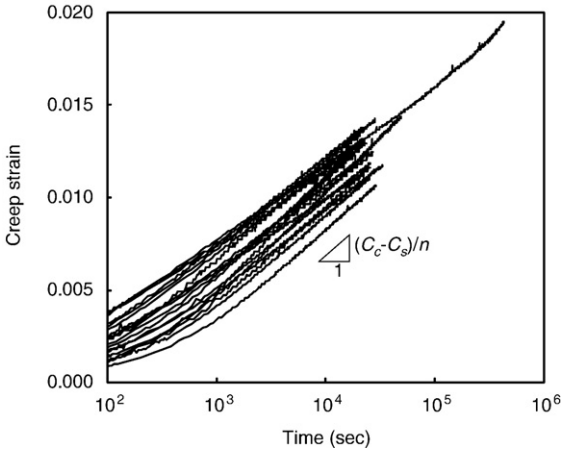

Fig. 5. Collection of creep strains as a function of log time. The creep strains shown here are those at pressures above 30 MPa.

One problem with this approach is that we need to know the initial preconsolidation pressure to evaluate p_o after the shale experiences some strain hardening. Because a precise value of the initial preconsolidation pressure of the dry shale is not available, an accurate estimation of c_o value is not possible. Thus, we will assume that the shale underwent near full consolidation during the creep stage just before we increased the pressure to the next step. Fig. 6 shows the result for estimating c_o. Because 5-MPa steps were used in our experiments, we compare the computed values of $D(p/(p-5))^n$ for all pressure levels used in the creep experiments (the abscissa) with the values of $c_oDe^{D(\varepsilon_\infty^{vp}-\varepsilon_o^{vp})}$ obtained from best-fit equations on creep strain versus time curves (the ordinate). The slope of the best-fit line is c_o, which is determined to be 1.03×10^{-7}. Thus, the viscoplastic constitutive law for the dry frame of GOM shale under hydrostatic pressure has its final form of

$$\dot{\varepsilon}^{vp}=1.03\times10^{-7}\left(\frac{p}{p_o}\right)^{38\pm4}. \tag{14}$$

7. Implication and discussion

Wetting and saturation are known to alter shales and affect their compaction behavior (Chenevert and Amanullah, 2001), and the rate-dependency parameter determined from dry shale tests may not be directly used in predicting in situ shale properties. However, the utilization of the simple plastic model combined with the viscoplastic theory gives some insight into the mechanism of shale compaction. Two basic implications of the model presented above are as follows. First, time-dependent creep occurs in response of the evolution of preconsolidation pressure p_o that follows the normal compaction trend whenever the current pressure p exceeds p_o. Eq. (14) shows that as p_o increases with time toward p, the rate of creep strain diminishes as observed in typical creep strain–time curves. Second, the yield pressure increases with strain rates. The rate-dependency of yield stress depends on the value of the exponent n defined in Eq. (9); the lower n is, the higher rate-dependency is. This means that the rate-dependency of yield stress can be estimated from creep strain versus time curves, as their slope in log time scale is given by $1/D=(C_c-C_s)/n$. Based on Eq. (14), the increase in strain rate by an order of magnitude ($\times10$) raises the dynamic yield stress p by 6–7% ($=(10^{1/n}-1)\times100$). If we compare the strain rate in the laboratory and in the field, for example,

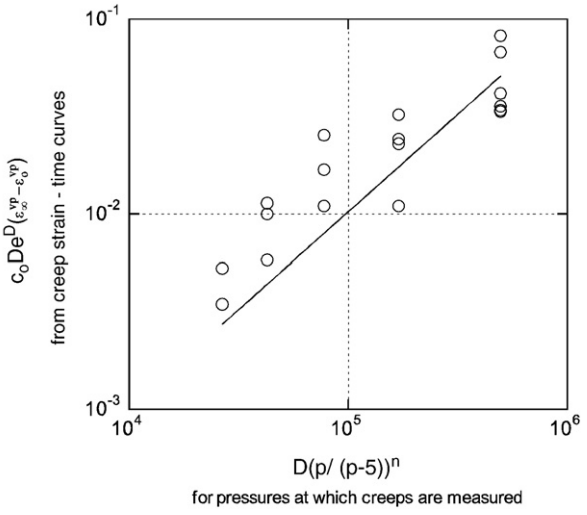

Fig. 6. Comparison of the coefficient $c_oDe^{D(\varepsilon_\infty^{vp}-\varepsilon_o^{vp})}$ determined numerically from the creep strain–time curve (plotted in the ordinate) and $D(p/(p-5))^n$ for pressures at which creeps were measured (plotted in the abscissa). The slope of the best-fit line is c_o, which is determined to be 1.03×10^{-7}.

the difference could be a factor of three or more, which could overestimate the yield stress in situ by at least ~20% or higher. Thus, in that case, the laboratory determined pressure and porosity relation may significantly overestimate the size of the yield surface (i.e., the position of the end-cap) in the field.

It should be noted again that time-dependent creep is an intrinsic nature of deformation in the dry frame of shale. The strain rate-dependency of rock strength (or yield stress) addressed in this study is associated with viscous creep. Time-dependent deformation due to pore pressure dissipation should be interpreted as a result of gradual changes in effective stress, which is an additional mechanism best addressed in terms of poroelasticity. For example, when effective stress increases by Δp in a normally consolidated formation with its preconsolidation pressure of p_o, the formation undergoes first an instantaneous poroelastic deformation, followed by viscous deformation of the shale matrix due to stress changes. Thus, the total strain ($\varepsilon^{\text{total}}$) is the sum of poroelastic strain (ε^{pe}) and time-dependent viscoplastic strain (ε^{vp}):

$$\varepsilon^{\text{total}}(\Delta p, t) = \varepsilon^{\text{pe}}(\Delta p) + \varepsilon^{\text{vp}}(\Delta p, t). \tag{15}$$

Here, from Eqs. (10) and (13), the viscoplastic strain can be written as

$$\varepsilon^{\text{vp}}(\Delta p, t) = \frac{1}{D}\ln\left(c_o D\left(\frac{p_o + \Delta p}{p_o}\right)^n t + 1\right). \tag{16}$$

Because the viscoplastic constitutive model is derived for hydrostatic loading, it may not be directly applicable to the stress conditions in the field where stress path may be more similar to uniaxial compaction. However, if the change in effective stress is only due to pore pressure change, i.e. hydrostatic, the model may still be applicable in situ. Furthermore, as long as the viscoplastic theory used in this study is valid, the material constants evaluated here are expected to be valid for any arbitrary stress history. Application of the determined material parameters to the generalized stress conditions requires the use of the more general form of constitutive law such as that given in Eq. (8). In that case, additional parameters such as the slope of the critical state line M should be determined, which is related to the internal friction coefficient based on Mohr–Coulomb theory of yielding (Desai and Siriwardane, 1984).

There are several applications for which the type of viscoplastic model presented here can be useful. The most direct application would be a more precise estimation of porosity (and yield stress) evolution during burial or due to perturbations associated with drilling or production from sands adjacent to weak shales and resultant subsidence. Similarly, incorporation of the type of constitutive law presented could be helpful in improved estimation of pore pressure prediction from laboratory uniaxial consolidation experiments (Stump and Flemings, 2002; Saffer, 2003).

8. Conclusions

We employed the modified Cam-clay plastic yield model incorporated into the Perzyna's viscoplasticity framework in order to find a relatively simple model that describes the creep properties of the dry skeleton of the GOM shale. The model describes the creep strain as a function of logarithm of time, which is in agreement with our hydrostatic pressure experimental results. By fitting experimental creep–time curves and comparing them with the model-derived constitutive equation, parameters necessary to define the viscoplastic model were determined for the shale. The determined models indicate that as strain rate increases by an order of magnitude, the yield pressure of the hydrostatically loaded shale rises by 6–7%. Because of a wide variation of the strain rates in the laboratory and in situ, the model can provide a more accurate prediction of yield pressure as well as porosity change that depend on strain rate.

Acknowledgments

This work was supported by the Stanford Rock Physics and Borehole Geophysics consortium. Comments made by Paul Hagin greatly enhanced the quality of this paper.

References

Adachi, T., Oka, F., 1982. Constitutive equations for normally consolidated clay based on elasto-viscoplasticity. Soils Found. 22, 57–70.
Bjerrum, L., 1967. Engineering geology of Norwegian normally consolidated marine clays as related to settlements of buildings. Geotechnique 17, 81–118.
Chang, C., Zoback, M.D., 2009. Viscous creep in room-dried unconsolidated Gulf of Mexico shale; experimental results. J. Petrol. Sci. Eng. 69, 239–246.
Chang, C., Moos, D., Zoback, M.D., 1997. Anelasticity and dispersion in dry unconsolidated sands. Int. J. Rock Mech. Min. Sci. 34: Paper No. 48.
Chenevert, M.E., Amanullah, M., 2001. Shale preservation and testing techniques for borehole-stability studies. SPE Drill. Complet. 16, 146–149.
Cogan, J., 1976. Triaxial creep tests of Opohonga limestone and Ophir shale. Int. J. Rock Mech. Min. Sci. 13, 1–10.
Desai, C.S., Siriwardane, H.J., 1984. Constitutive Laws for Engineering Materials, With Emphasis on Geologic Materials. Prentice-Hall, New Jersey. 468 pp.
Fodil, A., Aloulou, W., Hicher, P.Y., 1997. Viscoplastic behaviour of soft clay. Geotechnique 47, 581–591.
Hagin, P.N., Zoback, M.D., 2004a. Viscous deformation of unconsolidated reservoir sands; part 2, linear viscoelastic models. Geophysics 69, 742–751.
Hagin, P.N., Zoback, M.D., 2004b. Viscoplastic deformation in unconsolidated reservoir sands (Part 1): Laboratory observations and time-dependent end cap models. SPE/ARMS 04-567.
Hornby, B.E., 1998. Experimental laboratory determination of the dynamic elastic properties of wet, drained shales. J. Geophys. Res. 103, 29945–29964.
Karig, D.E., 1993. Uniaxial reconsolidation tests on porous sediments: mudstones from site 897. In: Whitmarsh, R.B., Sawyer, D.S., Klaus, A., Masson, D.G. (Eds.), Proceedings of the Ocean Drilling Program, Scientific Results, 149, pp. 363–373.
Katona, M.G., 1984. Evaluation of a viscoplastic cap model. J. Geotech. Eng. 110, 1106–1125.
Kutter, B.L., Sathialingam, N., 1992. Elastic–viscoplastic modelling of the rate-dependent behaviour of clays. Geotechnique 42, 427–441.
Namikawa, T., 2001. Delayed plastic model for time-dependent behaviour of materials. Int. J. Numer. Anal. Methods Geomech. 25, 605–627.
Ostermeier, R.M., 1995. Deepwater Gulf of Mexico turbidites; compaction effects on porosity and permeability. SPE Form. Eval. 10, 79–85.
Perzyna, P., 1963. The constitutive equations for rate sensitive plastic materials. Q. Appl. Math. 20, 321–332.
Roscoe, K.H., Burland, J.B., 1968. On the generalized stress–strain behaviour of wet clay. In: Heyman, J., Leckie, F.P. (Eds.), Eng. Plast. 535–609.
Roscoe, K.H., Schofield, A.N., Thurairajah, A., 1963. Yielding of clays in states wetter than critical. Geotechnique 13, 211–240.
Saffer, D.M., 2003. Pore pressure development and progressive dewatering in underthrust sediments at the Costa Rican subduction margin: comparison with northern Barbados and Nankai. J. Geophys. Res. 108 EPM9-1-16.
Schutjens, P.M.T.M., Hanssen, T.H., Hettema, M.H.H., Merour, J., de Bree, P., Coremans, J.W.A., Helliesen, G., 2004. Compaction-induced porosity/permeability reduction in sandstone reservoirs: data and model for elasticity-dominated deformation. SPE Reserv. Evalu. Eng. 7, 202–216.
Stump, B.B., Flemings, P.B., 2002. Consolidation state, permeability, and stress ratio as determined from uniaxial strain experiments on mudstone samples from the Eugene Island 330 area, offshore Louisiana. AAPG Mem. 76, 131–144.
Vermeer, P.A., Neher, H.P., 1999. A soft soil model that accounts for creep. In: Brinkgreve, R.B.J. (Ed.), Proceedings of the International Symposium "Beyond 2000 in Computational Geotechnics", pp. 249–261.
Yin, J.H., Graham, J., 1999. Elastic viscoplastic modelling of the time-dependent stress–strain behaviour of soils. Can. Geotech. J. 36, 736–745.